Optimization of highly concentrated dispersions of multi-walled carbon nanotubes with emphasis on surfactant content and carbon nanotubes quality

Maël Pontoreau, Emmanuel Le Guen, Christine Bourda, Jean-François Silvain

Optimization of highly concentrated dispersions of multi-walled carbon nanotubes with emphasis on surfactant content and carbon nanotubes quality

Maël PONTOREAU[a,*], Emmanuel LE GUEN[b], Christine BOURDA[b], Jean-François SILVAIN[a,c]

[a] CNRS, Univ. Bordeaux, Bordeaux INP, ICMCB, UMR 5026, F-33608, Pessac, France

[b] METALOR Technologie SAS, F-28190, Courville-sur-Eure, France

[c] Department of Electrical and Computer Engineering, University of Nebraska-Lincoln, Lincoln, NE, 68588, USA

*Corresponding author. + 33 6 89 12 36 40, Mael-Pontoreau@protonmail.com

Abstract

Optimized multi-wall carbon nanotubes (MWNT) suspensions in aqueous solution have been obtained by joint use of ultrasonification and surfactant. A simple experimental procedure has been established to efficiently evaluate the dependence of the surfactant concentration on the MWNT concentration stable in suspension. The study of 3 different surfactants and MWNT provided by 3 suppliers showed that a threshold surfactant concentration exists above which the MWNT concentration is maximum. Furthermore, it is demonstrated that the maximum MWNT concentration achievable varies from 0.50 to 7.5 g/L depending mainly on quality of the MWNT determined by Raman spectroscopy analysis.

1. Introduction

Over the past three decades, carbon nanotubes (CNT) have drawn more and more attention of researchers all over the world. Among CNT, single-walled carbon nanotubes (SWNT) are described as a single layer of graphite rolled into a cylinder whereas multi-walled carbon nanotubes (MWNT) consist of sets of concentric cylindrical graphite shell. Typically, CNT are known as a carbon nanomaterial with a nanometric diameter and a microscopic length. Due to their outstanding mechanical, thermal, electrical and optical properties [1]–[5], the development of CNT-based composites may find wide range of applications in polymer industry [6], electronic components [7] or field emission devices [8]. More recently, the use of this carbon nanomaterial in the preparation of nanofluids with improved thermophysical properties is under investigation for applications in heat exchangers [9].

However, as-produced CNT mainly exist as bundles arising from both chemical and physical entanglement of CNT due to van der Waals interactions between the tubes [10] and the high aspect ratio of CNT respectively [11]. In order to obtain homogeneous dispersion of CNT in nanotube-based composite materials and nanofluids, one of the key challenges is to de-agglomerate the CNT.

Nowadays, solution based processing is the main route available which results in stable suspensions of CNT in which CNT are individualized [12]. More precisely, most of the suspensions of CNT are obtained in aqueous solution by the joint use of ultrasonic treatment and organic species (polymers, surfactants …). On one hand, cavitation induced by the ultrasonic treatment [13] de-agglomerates the bundles of CNT [14]. On the other hand, adsorption of surfactant or polymers on the surface of CNT introduces repulsive interactions between the CNT surpassing the van der Waals interactions and preventing their re-

agglomeration in solution. The adsorption of organic species on the surface of CNT is known as non-covalent functionalization and modifies the interfacial properties of CNT without compromising their structures unlike covalent functionalization, which consists in linking functional groups onto the CNT' surface [15], [16].

Even if the adsorption mechanisms of the surfactants on the CNT surface are under investigations [17], the ability of surfactants to stabilize CNT in suspension has been studied multiple times. Different surfactants have been used such as sodium dodecyl sulphate (SDS) [17]–[21], cetrimonium bromide (CTAB) [22] and Triton X-100 [23]–[25]. Some studies show significant differences in CNT' stabilization depending on the surfactant's nature and concentration [12], [25]–[27]. Measurement of zeta potential depending on the pH value of the aqueous solution is commonly used in these studies [21], [26], [28].

Moreover, efforts have been devoted optimizing the time and the power of the ultrasonic treatment. Actually, transmission electron microscopy (TEM) and Raman spectroscopy analysis showed that « sonication induced CNT cutting » occurs [29] and the structure of CNT is damaged during the ultrasonic treatment [30], [31]. By using the results obtained by UV-Vis spectroscopy, the duration of the ultrasonic treatment has been reduced as much as possible in order to preserve the integrity of CNT while obtaining a high concentrated CNT suspension [18], [32]. UV-Vis spectroscopy is usually used to compute the concentration of the suspensions based on previous experiments carried out on MWNT [33]. At that time, few studies have been conducted on the influence of the CNT characteristics on CNT suspension. Contradictory reports exist on the effect of the length of the CNT [34], [35].

Therefore, the objectives of our study are to provide details on the dispersion of MWNT in aqueous surfactant solutions using 3 surfactants and 3 MWNT of different morphologies. An emphasis is placed on the mass ratio between surfactant and MWNT prior to ultrasonic treatment as well as the determination of the concentration of the surfactant and MWNT stable in suspension.

2. Experimental

2.1 Materials

Three types of purified MWNT have been studied, namely, NC7000^{TM} provided by Nanocyl®, MWNT provided by US Research Nanomaterials® and MWNT GCM331 provided by Carbon Nanotubes Plus®. The manufacturer's specifications of the MWNT are grouped in

Table 1. For ease of understanding, MWNT will be referred MWNT1, MWNT2 and MWNT3 respectively.

Suppliers	Synthesis method	Purity (wt.%)	Length (μm)	Outside diameter (nm)	Surface Area (m^2/g)
MWNT1 (Nanocyl®)	CCVD	> 90%	1 – 2	9 – 10	250 – 300
MWNT2 (US Research Nanomaterials®)	CCVD	> 95%	10 – 30	10 – 20	> 200
MWNT3 (Carbon Nanotubes Plus®)	CCVD	> 98%	10 – 30	10 – 20	> 150

Table 1 : Manufacturer's specifications of the MWNT

The 3 surfactants used are SDS (Fisher Scientific ®), CTAB (Serva®) and Triton X-100 (Sigma-Aldrich®) with purity higher than 95%. The main characteristics of the surfactant used are specified in Table 2. All solutions were prepared in 18 MΩ-deionized water.

Surfactant	Chemical formula	Type of surfactant	CMC at 25°C (mg/mL)	HLB at 20°C
SDS	$C_{12}H_{25}NaSO_4$	Anionic	2 – 2.9	40
CTAB	$C_{19}H_{42}BrN$	Cationic	0.35	18
Triton X-100	$C_8H_{17}C_6H_4(OC_2H_4)_{9\text{-}10}OH$	Non-ionic	0.12-0.56	13.5

Table 2 : Characteristics of the used surfactant (CMC: critical micelle concentration, HLB: hydrophilic-lipophilic balance)

2.2 Dispersion of MWNT in various surfactants solution

In order to compare the suspensions of MWNT depending on the surfactant's concentration, dispersions of MWNT were prepared by adding 750 mg of MWNT to 75 mL of an aqueous surfactant solution. The initial concentration of MWNT is thus kept constant for all experiments. This aqueous solution contains the surfactant (either SDS or CTAB or Triton X-100) at concentrations spanning from 0 to 10 mg/mL. All three surfactants were used with MWNT2 whereas MWNT1 and MWNT3 were used only with SDS.

All resulting aqueous solutions were sonicated for 1 h with an ultrasonic homogenizer (Bandelin Sonopuls® UW2200) with active intervals of 0.1 s, passive intervals of 0.9 s, amplitude fixed at 50% and a power equals to 200 W. Subsequently, the solutions were centrifuged for 5 min at 2680 g_0 in order to bring bundles as well as residual catalyst particles to the bottom of the centrifuge tubes [17], [19], [25], [27], [36]. The supernatants were selected and further characterized. For some characterizations, the supernatants were dried at 60 °C overnight. Each suspension will be referenced in function of the MWNT batch and surfactant used as well as the initial mass ratio surfactant/MWNT. For example MWNT2-SDS(0.5) refers to a MWNT2 suspension with SDS concentration equals to 5 mg/mL.

2.3 Investigation methods

2.3.1 Characterization of debundling

To confirm debundling of the MWNT in the supernatant, scanning electron microscopy (SEM) and TEM were performed using Tescan® Vega II and Jeol® JEM 1400+ respectively. For each analysis, a droplet of the suspension was dried on the appropriate substrates (TEM grid cover with carbon film).

2.3.2 Characterization of suspension's content

Similarly to previous studies, the debundling of MWNT was characterized using UV-Vis spectrophotometer (Varian® Cary 5000) operating between 250-800 nm. In order to establish a relationship between the amount of suspended MWNT and the intensity of the corresponding absorption spectrum, the samples were diluted by a certain factor. Same spectroscopy cells measuring 10 mm have been used for all measurements. From 250 to 800 nm, the absorption of aqueous solutions of each surfactant was measured to be zero relative to the water used for baseline correction.

By drying the supernatant at 60 °C, solid particles consisting of a mixing of MWNT and surfactant can be collected. For each suspension, total concentration of MWNT and surfactant in the supernatant was computed by drying a specific volume of the supernatant and weighing the collected solid particles [15]. Moreover, quantification of carbon and hydrogen – using a CHNS elemental analyzer (Thermo Fisher Scientific®) – was systematically performed to determine the relative amount of MWNT and surfactant in the collected solid particles. These measurements were repeated at least 3 times with about 3 mg of particles collected each time. Pristine MWNT and surfactants were measured as references after being dried at 60 °C

overnight. Standard deviations of the different measurements are used to compute absolute uncertainty.

A thermal gravimetric analyzer (Setaram® TAG 24) was used as second characterization technique to confirm the ratio between MWNT and surfactants. The thermogravimetric analysis (TGA) were performed between 25 to 600 °C at a heating rate of 5 °C/min under argon atmosphere.

2.3.3 Characterization of CNT's integrity

MWNT morphology was investigated by Raman spectroscopy (Horiba® LabRAM HR). The excitation source was a He-Ne laser (632.8 nm) and the power was kept below 1 mW to avoid local heating of the sample. The band fitting of the spectra was carried out using Lorentzian and Gaussian functions as reported elsewhere [37].

3. Results and discussion

3.1 Debundling of MWNT

Firstly, it had be verified experimentally that the debundling of MWNT can only occur by the joint use of an ultrasonic treatment and a surfactant. Figure 1 shows observations of different MWNT2 aqueous solutions, some of which have undergone US treatment with or without a SDS concentration of 10 mg/mL. Instead of US treatment, aqueous solutions have been magnetically stirred at 500 rpm for 1 h. After being vertically stored for 3 days, it appears that stable suspension is only obtained by the combination of physical and chemical method. Without surfactant (cf. Figure 1 b), MWNT2 are exfoliated but agglomerate in solution. Agglomeration of MWNT2 is prevented by the surfactant adsorbed on MWNT's surface (cf. Figure 1 d). Even after the centrifugation step, the supernatant remains opaque which means that a significant amount of MWNT2 stays in suspension in the aqueous solvent.

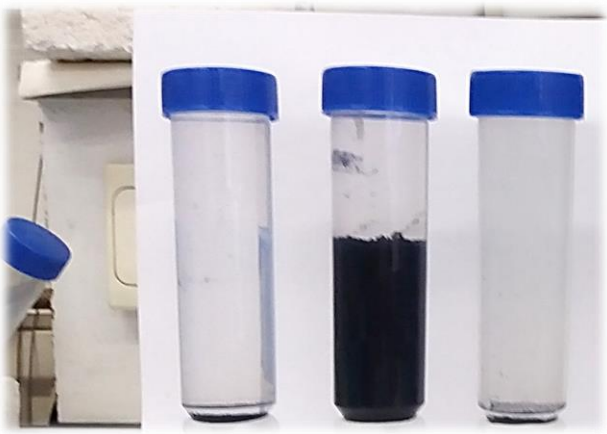

a) b) c) d)

Figure 1 : MWNT2 aqueous solutions after being vertically stored for 3 days a) without US treatment and surfactant b) only with US treatment c) only with surfactant d) with both US treatment of surfactant

SEM and TEM micrographs were taken from MWNT2-SDS(1) using dilute droplet of surfactant after US treatment and the centrifugation step and compared to the initial MWNT2 without US treatment (cf. Figure 2 and Figure 3). Initially, MWNT are extremely entangled forming macroscopic and microscopic bundles (cf. Figure 2 a et Figure 3 a). By the joint use of US treatment and surfactant, MWNT are deagglomerated and are individualized in suspension (cf. Figure 2 b and Figure 3 b). The length of collected MWNT is much smaller compared to the length announced by the supplier, which is due to sonication induced MWNT cutting. No statistical results are shown in this study. Similar microscopic analyses have been carried out on MWNT1 and MWNT3 with similar results.

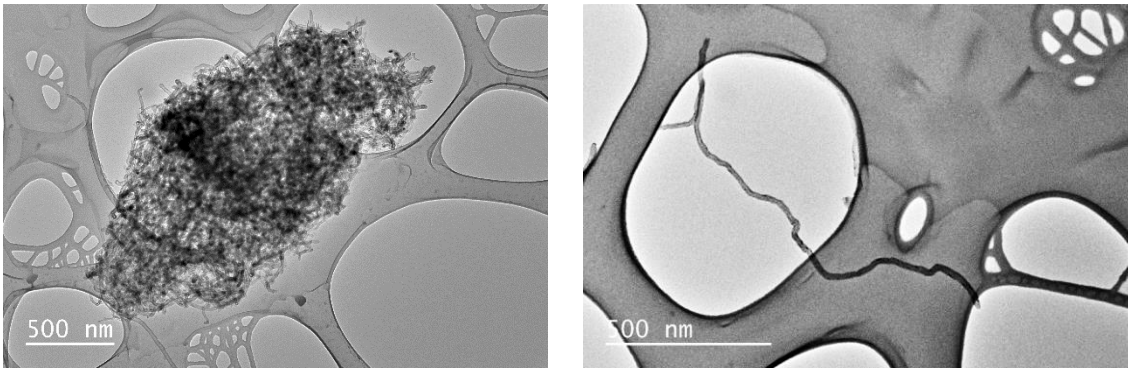

a) b)

Figure 2 : TEM micrographs of a) raw MWNT2 b) MWNT2-SDS(1) (droplet diluted by a factor 50)

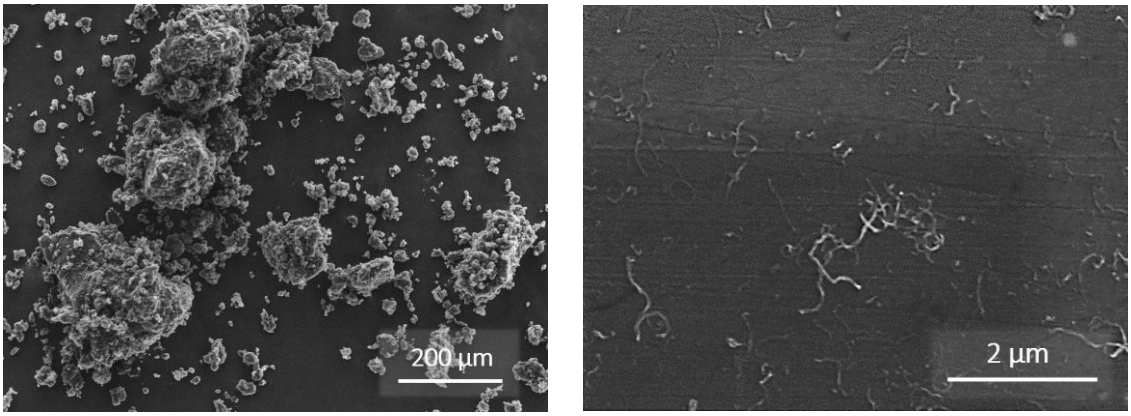

a) b)

Figure 3 : SEM micrographs of a) raw MWNT2 b) MWNT2-SDS(1) (droplet diluted by a factor 50)

3.2 Comparison of MWNT suspensions

3.2.1 UV-Vis spectroscopy analysis

As reported elsewhere, debundled MWNT dispersed in solution are active in the UV-Vis region and exhibit characteristic bands corresponding to additional absorption due to 1D van Hove singularities [32], [38]. Therefore, UV-Vis spectroscopy can be used to detect and quantify MWNT in suspension. Figure 4 illustrates UV-Vis spectra of MWNT2-SDS suspensions made with different SDS/MWNT initial mass ratios. Similarly to other studies, a maximum around 250 nm can be noticed which means that the suspensions are composed of individual MWNT.

However, the maximum absorbance of MWNT suspensions varies significantly depending on the initial surfactant's concentration. Firstly, the absorbance increases gradually with the surfactant/MWNT mass ratio. In a second time, the absorbance remains interestingly constant. This result means that a maximum concentration of CNT in solution is reached when the mass ratio is above 0.3. UV-Vis spectra of all other MWNT suspensions exhibit similar behavior. Figure 5 and Figure 6 plot the absorbance measured at 500 nm for MWNT-SDS suspensions and MWNT2-surfactant suspensions respectively. Depending on initial surfactant/MWNT mass ratio, a certain mass ratio exists above which the absorbance – and consequently the concentration of MWNT in suspension – reaches a maximum. Consequently, these results show that, above a certain mass ratio MWNT/surfactant, the surface of all the MWNT, deagglomerated by the US treatment, is saturated with surfactant molecules. A further

increase of the concentration of surfactant in solution does not affect the MWNT. These threshold mass ratios depend on both the MWNT and the surfactant used. They are typically ranging from 0.2 to 0.5. It can be noticed that these threshold values do not correlate with the CMC of the surfactants.

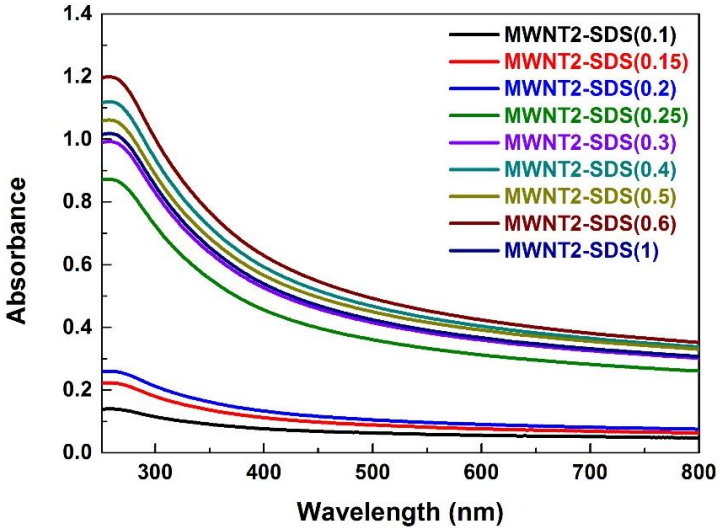

Figure 4 : Evolution of the absorbance of MWNT2-SDS suspension in function of the initial mass ratio MWNT2/SDS

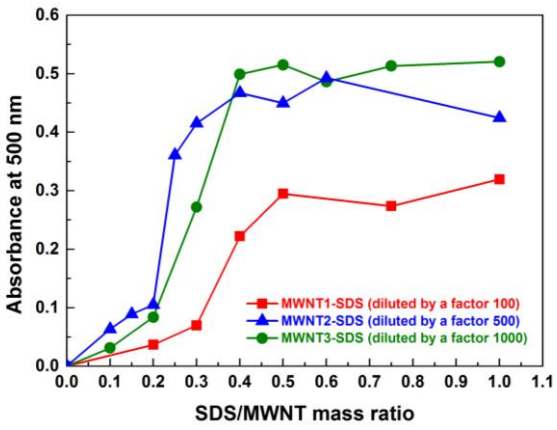

Figure 5 : Evolution of the absorbance at 500 nm of suspensions of MWNT in function of the MWNT and of initial mass ratio MWNT/SDS

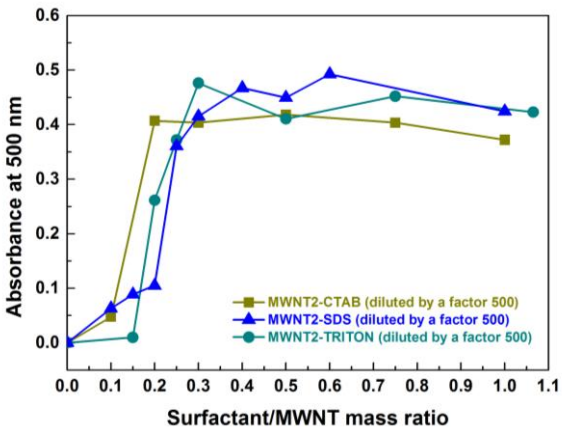

Figure 6 : Evolution of the absorbance at 500 nm of MWNT 2 suspensions in function of the surfactant and of initial mass ratio MWNT/surfactant

For a given MWNT suspension, the maximum absorbance measured reflects the maximum MWNT concentration in suspension. Depending on the MWNT, the dilution factor equals to 100, 500 and 1000 for MWNT1, MWNT2 and MWNT3 respectively are used. As the absorbance at 500 nm for the suspensions MWNT2-SDS and MWNT3-SDS are similar, despite

the different dilution factors, the maximum MWNT concentration in suspension are significantly different. Using Beer-Lambert law, maximum MWNT concentration in the suspension can be compared.

Assuming that the extinction coefficient is the same for each MWNT batch, taking account of the dilute factor and using the mean absorbance of the suspensions for a mass ratio above 0.5, maximum MWNT concentrations of all suspensions compared to MWNT2-SDS suspensions can be computed following the following equation :

$$\frac{C_{MWNT\ max\ (Suspension)}}{C_{MWNT\ max\ (MWNT2-SDS)}} = \frac{A_{500\ nm\ (Suspension)} * \text{Dilute factor}_{(Suspension)}}{A_{500\ nm\ (MWNT2-SDS)} * \text{Dilute factor}_{(MWNT2-SDS)}}$$

Table 3 shows the mean absorbance at 500 nm of each suspension for a mass ratio above 0.5 as well as the ratio of the maximum concentration of MWNT in each suspension to the maximum concentration of MWNT in MWNT2-SDS suspensions.

Suspensions (dilute factor)	MWNT2-SDS (x500)	MWNT1-SDS (x100)	MWNT3-SDS (x1000)	MWNT2-CTAB (x500)	MWNT2-TRIT (x500)
Mean absorbance at 500 nm (A_{500nm})	0.46 ± 0.05	0.30 ± 0.03	0.51 ± 0.02	0.40 ± 0.02	0.43 ± 0.02
$\frac{C_{MWNT\ max\ (suspension)}}{C_{MWNT\ max\ (MWNT2-SDS)}}$	1 ± 0.11	0.13 ± 0.01	2.22 ± 0.09	0.87 ± 0.04	0.93 ± 0.04

Table 3 : Ratio of maximum concentrations of MWNT for the different suspensions according to the Beer Lambert law

In this Table *3*, only the ratio of maximum MWNT concentrations is presented. Actual concentrations of MWNT are determined by the following experimental method. Further discussions of the maximum concentration measured by each method will be done.

3.2.2 Weighing method

By drying and weighing precise volumes of suspensions of MWNT, evolutions of the total concentration of surfactant and MWNT in function of initial surfactant/MWNT mass ratio have been computed for each suspension (cf. Figure 7 and Figure 8).

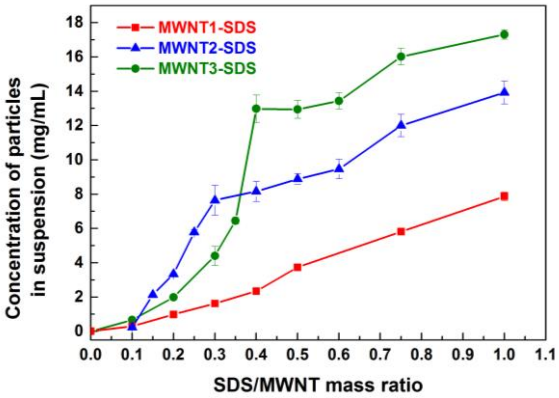

Figure 7 : Evolution of the mass of the collected particles in function of the initial mass ratio SDS/MWNT for MWNT-SDS suspensions

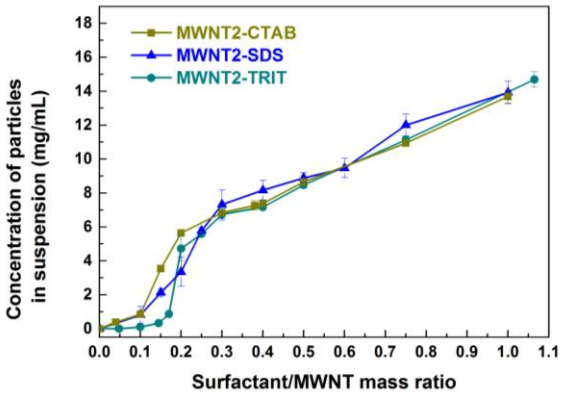

Figure 8 : Evolution of the mass of the collected particles in function of the initial mass ratio surfactant/MWNT2 for MWNT2-surfactant suspensions

For each suspension, these evolutions can be divided into two parts. Firstly, from 0 to a certain surfactant/MWNT mass ratio, the concentration of collected particles soars. Experimentally, this increase can be seen as supernatant becomes darker and darker which means that the concentration of MWNT being suspended increases. Secondly, when the mass ratio further increases, the increase of concentration becomes slighter. In accordance with the UV-Vis spectroscopy measurements, the shape of the graphs demonstrates that the concentration of MWNT remains stable in the supernatant above a threshold surfactant/MWNT mass ratio. Indeed, the threshold mass ratios are similar to those determined by UV-Vis spectroscopy measurements. The slight rise of concentration computed is only due to a further increase of the concentration of the surfactant in the supernatant.

For the suspensions MWNT1-SDS, the threshold mass ratio is unclear because of the low concentration of MWNT. However, it can be noticed that total concentration of SDS and MWNT in the supernatant is systematically lower than the initial surfactant concentration. It means that some SDS molecules are adsorbed on the surface of the bundles of MWNT at the bottom of the centrifugation tubes. In the case of MWNT1-SDS, the amount of surfactant adsorbed on the surface of MWNT would not be sufficient to prevent major bundling of MWNT in suspension and, thus, MWNT sedimentation upon centrifugation.

3.3 Relative proportion of SDS and MWNT in the suspension

Further investigations have been carried out to compute the actual concentrations of MWNT and of surfactant for each suspension of MWNT.

The hydrogen content of collected particles after drying has been measured using a CHNS elemental analyzer. Indeed, all three surfactants contain a significant amount of hydrogen whereas the amount of hydrogen in the MWNT is extremely low. Consequently, the measurement of the hydrogen content of the collected particles after drying leads to the computation of relative amount of MWNT and of surfactant. Due to low MWNT concentration in the MWNT1-SDS suspensions, it is not possible to compute the mass fraction of SDS thanks to the elemental analyzer. Actually, the amount of SDS is so high that the amount of hydrogen measured is too close to the amount of hydrogen in the SDS. Moreover, TGA analysis have been also used to quantify the proportion of MWNT2 and SDS in the dried MWNT2-SDS suspensions. Under inert atmosphere, MWNT are very stable until 600 °C whereas SDS decomposes significantly after 200 °C. Consequently, the height of mass loss above 200 °C can be related to the mass fraction of SDS. All the TGA curves obtained for MWNT2-SDS suspensions are shown in Figure 9.

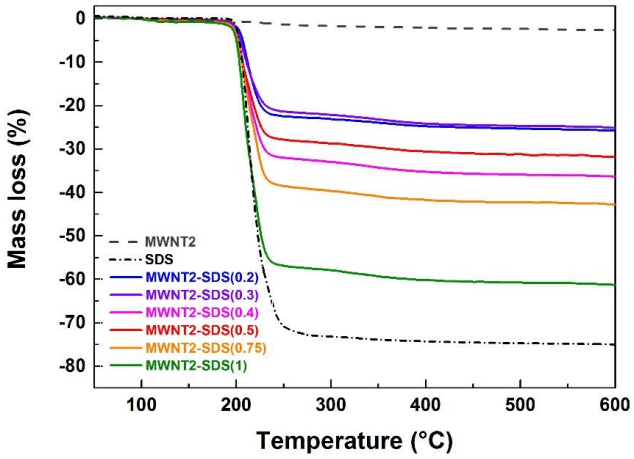

Figure 9 : TGA analysis of MWNT2-SDS suspensions (5 °C/min, Ar)

The relative proportion of SDS and CNT have been computed by an adapted lever rule for each technique:

- For elemental composition measurement :

$$\%_{wt}Surfactant_{sample} = \frac{\left(\%_{wt}H_{sample} - \%_{wt}H_{MWNT}\right)}{\left(\%_{wt}H_{Surfactant} - \%_{wt}H_{MWNT}\right)} * 100$$

- For TGA measurement (computation for the mass loss at 400, 500 and 600 °C) :

$$\%_{wt}Surfactant_{sample} = \frac{\left(\Delta m_{sample} - \Delta m_{MWNT}\right)}{\left(\Delta m_{Surfactant} - \Delta m_{MWNT}\right)} * 100$$

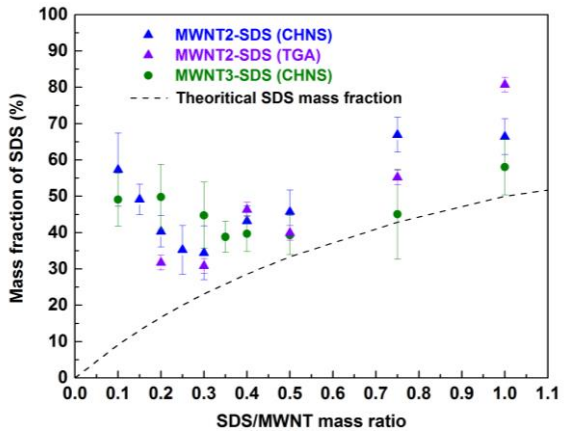

Figure 10 : Evolution of the mass fraction of SDS in function of the initial mass ratio SDS/MWNT for MWNT-SDS suspensions

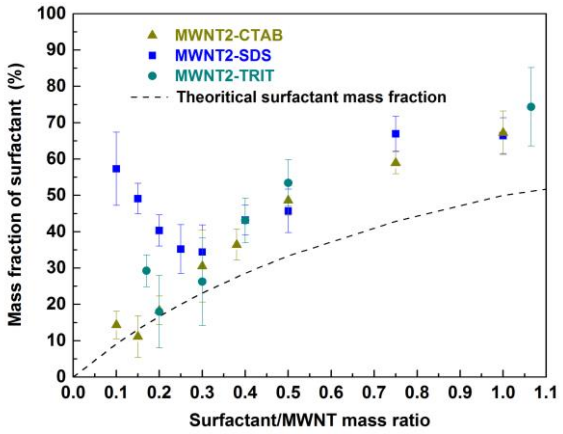

Figure 11 : Evolution of the mass fraction of surfactant in function of the initial mass ratio surfactant/MWNT2 for MWNT2-surfactant suspensions

Figure 10 and Figure 11 show the evolutions of surfactant mass fraction deduced from TGA and hydrogen content measurement for all the suspensions. The evolutions of the surfactant mass fractions are compared to the initial surfactant mass fraction before the US treatment.

The graphs show that surfactants' mass fractions are systematically superior to initial mass fractions. Generally, the mass fraction of surfactant decreases in a first time before increasing significantly from an initial mass ratio corresponding approximately to those determined by the two previous characterization techniques. This observation is once again consistent with the view that, above a certain initial surfactant/MWNT mass ratio, only the concentration of surfactant increases in the supernatant.

3.4 Evolution of the concentration of MWNT and surfactant in the supernatant

Combining the total concentration of surfactant and MWNT deduced by weighing with the mass fraction of surfactant, the evolution of MWNT and surfactant concentrations can be computed as shown in Figure 12 and Figure 13.

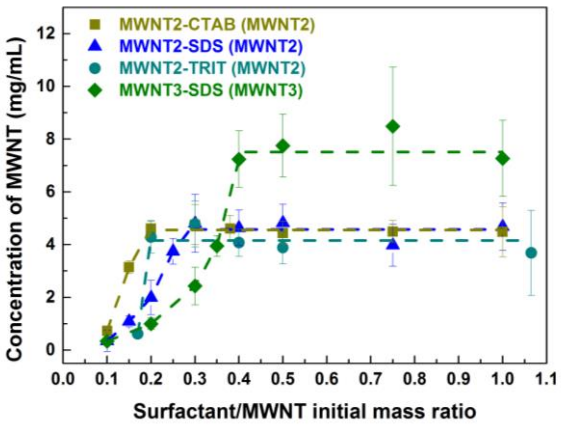

Figure 12 : Evolution of the suspended MWNT concentration in function of the initial mass ratio Surfactant/MWNT

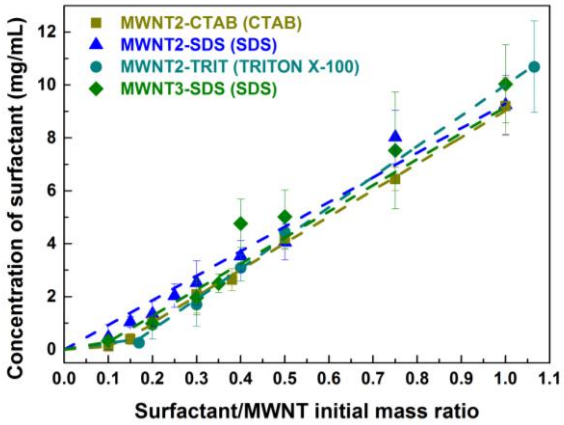

Figure 13 : Evolution of the surfactant concentration in the suspensions in function of the initial mass ratio Surfactant/MWNT

For each MWNT suspension, the concentration of surfactant increases linearly in function of the initial mass ratio. Concerning the MWNT concentration, it increases until initial mass ratio reaches a certain value. Then, above these threshold values, the MWNT concentration remains stable.

At the threshold value, the surface of the MWNT are fully covered by surfactant molecules and the repulsive interactions between MWNT permit to maintain a certain amount of MWNT in suspension. Considering that CNT are nanomaterials exhibiting huge surfaces, the concentration of surfactant molecules needed is logically higher than the CMC of a given surfactant. Once the MWNT are fully covered by surfactant, the MWNT concentration is not influenced by a further increase of the concentration of surfactant. Consequently, optimized suspensions highly concentrated in MWNT and weakly concentrated in surfactant can be obtained following the procedure described in this paper. For example, MWNT2-SDS(0.3) and MWNT3-SDS(0.4) are considered as optimized suspensions.

Linear fitting, with slope equals to 0, have been performed in order to determine the MWNT' maximum concentration for each suspension. Table 4 resumes the maximum MWNT concentrations for each type of suspension:

Suspensions	MWNT2-CTAB	MWNT2-SDS	MWNT2-TRIT	MWNT3-SDS
Maximum concentration of suspended MWNT (mg/mL)	4.56 ± 0.04	4.57 ± 0.16	4.15 ± 0.14	7.51 ± 0.22

Table 4 : Maximum MWNT concentrations of the different MWNT suspensions

The evolutions of the computed MWNT concentration are therefore consistent with the absorbance of the suspension measured by UV-Vis spectroscopy. MWNT3-SDS suspensions are the most concentrated suspensions. The ratio of the maximum MWNT concentration of MWNT3-SDS suspension to MWNT2-SDS equals to 1.64 ± 0.11, which is relatively close to ratio computed by UV-Vis spectroscopy (2.22 ± 0.09). Moreover, the suspensions elaborated with MWNT2 have approximately the same maximum concentration despite the fact that anionic, cationic and non-ionic surfactants were used. Therefore, for such highly concentrated MWNT suspension, this result indicates effectively that the stabilization effect would be mainly a steric one. According to the concentrations computed, the extinction coefficients of MWNT2 and MWNT3, at 500 nm, are equal to 48.7 ± 4.7 cm^2/mg (mean of MWNT2-SDS, MWNT2-CTAB and MWNT2-TRIT suspensions) and 67.9 ± 4.6 cm^2/mg, respectively. These values are consistent with those commonly used in the literature for low concentrated MWNT suspensions [39]–[42]. Using these two extinction coefficients, the maximum MWNT concentration of MWNT1-SDS is equal to 0.62 ± 0.12 mg/mL or 0.44 ± 0.07 mg/mL, respectively. For MWNT1-SDS suspensions, the optimized initial mass ratio equals to 0.5.

Therefore, in the frame of our study, the maximum achievable concentration of MWNT does not depend on the surfactant used but mainly on the batch of MWNT used. Indeed, all suspensions with MWNT2 have approximately the same maximum MWNT concentration. Moreover, using SDS as surfactant, the maximum MWNT concentration is significantly different for MWNT1, MWNT2 and MWNT3 despite the fact that MWNT2 and MWNT3 have the same initial length and diameter. However, the MWNT are not only defined by their initial length and diameter. Therefore, quality of the arrangement of the carbon atoms of the different batches of MWNT has been analyzed by Raman spectroscopy. It has to be mentioned that XPS analyses of the surface chemistry of the 3 different MWNT show almost identical results.

3.5 Raman spectroscopy analysis

Figure 14 shows the Raman spectra of pristine MWNT3. For each first order Raman spectra, five Raman bands of graphitic materials are identified and fitted by the procedure described elsewhere [37]. On the one hand, the G band (1580 cm^{-1}) corresponds to sp^2-C network. On the other hand, the D band (1350 cm^{-1}) and D' band (1620 cm^{-1}) are attributed to a double resonance Raman scattering mechanism and represent the defect in the C-lattice [37]. I (1170 cm^{-1}) and D" (1500 cm^{-1}) bands are attributed to disordered graphitic lattice and amorphous carbon respectively [43], [44]. The ratio I_D/I_G is commonly used to evaluate the amount of defects in the structure of CNT; the lower the ratio, the better the structure of the MWNT. Table 5 resumes the I_D/I_G ratios (average of five acquisitions) of as received MWNT and MWNT after US treatment with optimized MWNT/SDS mass ratio. Firstly, it can be noticed that the ratio I_D/I_G only slightly increases after the US treatment, which is typical of non-covalent functionalization.

Regarding the number of defects from one batch to another, a correlation can be established between the maximum achievable MWNT concentration and the quality of the structure of the MWNT. Whether on pure or suspended MWNT, MWNT3 presents the lowest ratio I_D/I_G and the highest maximum suspended MWNT concentration while MWNT1 presents the highest I_D/I_G and the lowest maximum suspended MWNT concentration. Actually, defects may disrupt the adsorption of SDS molecules on MWNT surface. Indeed, according to some reports, SDS molecules are adsorbed on the surface of the CNT by following the graphite network of CNT and forming supramolecular structures [23]. As defects detected by Raman spectroscopy are misarrangement of carbon atoms in the graphite network, one may think that defects disrupt the supramolecular organization of SDS around CNT. More generally, defects may disrupt organization of all kind of surfactants on CNT surface. Consequently, presence of defects lower the amount of surfactant that may adsorb on MWNT. With less surfactant, the repulsive interactions between MWNT decrease and thus the maximum concentration of MWNT in suspension.

Nevertheless, it should be stressed out that further investigations using a larger number of different MWNT batches are necessary to make a statistically relevant conclusion on the strength of the correlation between MWNT quality and the maximum achievable MWNT concentration. For example, adding defects by covalent functionalization on CNT surface and reproducing the experimental protocol presented in this article could be interesting. Nevertheless, it will have to be taken into account that misarrangement of carbon atoms on

CNT surface and functional groups are different types of defects which could have different impact on surfactant adsorption.

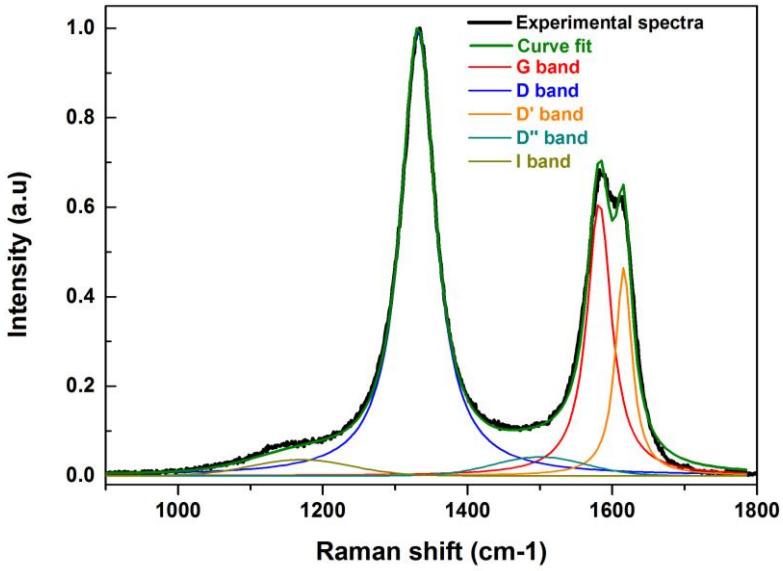

Figure 14 : First order Raman spectra of pristine MWNT3

	Pristine MWNT	Suspended MWNT
MWNT1	2.28 ± 0.17	2.40 ± 0.09
MWNT2	1.93 ± 0.10	2.03 ± 0.18
MWNT3	1.69 ± 0.12	1.67 ± 0.05

Table 5 : I_D/I_G ratio of pristine MWNT and of suspended MWNT (dried droplets)

4. Conclusion

We have investigated MWNT suspensions with three different surfactants and three batches of MWNT. The simultaneous use of ultrasonic treatment and surfactant successfully lead to the debundling of MWNT and to high concentrated MWNT suspensions. Moreover, a correlation has been established between the initial surfactant/MWNT mass ratio and the concentration of MWNT in suspension. It has actually been shown that threshold initial mass ratios exists above which a maximum concentration of suspended MWNT is achieved. A further increase of surfactant only induces an increase of surfactant content in suspension. Therefore, optimized MWNT suspensions have been defined for which the concentration of MWNT is maximum and the concentration of surfactant is minimum.

It has been proven that the maximum MWNT concentration depends mainly on the quality of the structure of the MWNT rather than their initial length, the surface composition

and the nature of the surfactant. Adsorption of surfactant may be disrupted due to the presence of structural defects. The maximum MWNT concentration achievable varies from 0.50 to 7.5 g/L depending mainly on quality of the MWNT.

The high concentrated MWNT suspensions may find many applications as nanofluids or as part of nanocomposites processes. Future studies could focus on demonstrating the strength of the correlation between MWNT quality and the maximum achievable MWNT concentration or on the optimization of the initial CNT nanotube concentration, the time and the power of ultrasonic treatment.

References

[1] S. Berber, Y. K. Kwon, and D. Tománek, "Unusually High Thermal Conductivity of Carbon Nanotubes," *Phys. Rev. Lett.*, vol. 84, no. 20, pp. 4613–4616, 2000, doi: 10.1103/PhysRevLett.84.4613.

[2] P. Kim, L. Shi, A. Majumdar, and P. L. McEuen, "Thermal Transport Measurements of Individual Multiwalled Nanotubes," *Phys. Rev. Lett.*, vol. 87, no. 21, p. 215502, 2001, doi: 10.1103/PhysRevLett.87.215502.

[3] M. J. Biercuk, S. Ilani, C. M. Marcus, and P. L. McEuen, "Electrical Transport in Single-Wall Carbon Nanotubes," in *Carbon Nanotubes: Advanced Topics in the Synthesis, Structure, Properties and Applications*, A. Jorio, G. Dresselhaus, and M. S. Dresselhaus, Eds. Berlin, Heidelberg: Springer Berlin Heidelberg, 2008, pp. 455–493.

[4] D. J. Yang, Q. Zhang, G. Chen, S. F. Yoon, J. Ahn, S. G. Wang, *et al.*, "Thermal conductivity of multiwalled carbon nanotubes," *Phys. Rev. B*, vol. 66, no. 16, p. 165440, 2002, doi: 10.1103/PhysRevB.66.165440.

[5] M. R. Falvo, G. J. Clary, R. M. Taylor, V. Chi, F. P. Brooks, S. Washburn, *et al.*, "Bending and buckling of carbon nanotubes under large strain," *Nature*, vol. 389, no. 6651, pp. 582–584, 1997, doi: 10.1038/39282.

[6] Z. Jin, L. Huang, S. H. Goh, G. Xu, and W. Ji, "Characterization and nonlinear optical properties of a poly(acrylic acid)–surfactant–multi-walled carbon nanotube complex," *Chem. Phys. Lett.*, vol. 332, no. 5, pp. 461–466, Dec. 2000, doi: 10.1016/S0009-2614(00)01294-X.

[7] K. Pietrzak, K. Frydman, D. Wójcik-Grzybek, A. Gładki, A. Bańkowska, and P. Borkowski, "Effect of Carbon Forms on Properties of Ag-C Composites Contact Materials," *Mater. Sci.*, vol. 24, no. 1, pp. 69–74, 2018, doi: 10.5755/j01.ms.24.1.17769.

[8] J. Koohsorkhi, Y. Abdi, S. Mohajerzadeh, H. Hosseinzadegan, Y. Komijani, and E. Asl. Soleimani, “Fabrication of self-defined gated field emission devices on silicon substrates using PECVD-grown carbon nano-tubes,” *Carbon*, vol. 44, no. 13, pp. 2797–2803, 2006, doi: 10.1016/j.carbon.2006.03.038.

[9] A. O. Borode, N. A. Ahmed, and P. A. Olubambi, “Surfactant-aided dispersion of carbon nanomaterials in aqueous solution,” *Phys. Fluids*, vol. 31, no. 7, p. 071301, 2019, doi: 10.1063/1.5105380.

[10] A. Thess, R. Lee, P. Nikolaev, H. Dai, P. Petit, J. Robert, *et al.*, “Crystalline Ropes of Metallic Carbon Nanotubes,” *Science*, vol. 273, no. 5274, pp. 483–487, 1996, doi: 10.1126/science.273.5274.483.

[11] J. Hilding, E. A. Grulke, Z. G. Zhang, and F. Lockwood, “Dispersion of Carbon Nanotubes in Liquids,” *J. Dispers. Sci. Technol.*, vol. 24, no. 1, pp. 1–41, 2003, doi: 10.1081/DIS-120017941.

[12] H. K. F. Cheng, Y. Pan, N. G. Sahoo, K. Chong, L. Li, S. Hwa Chan, *et al.*, “Improvement in properties of multiwalled carbon nanotube/polypropylene nanocomposites through homogeneous dispersion with the aid of surfactants,” *J. Appl. Polym. Sci.*, vol. 124, no. 2, pp. 1117–1127, 2012, doi: 10.1002/app.35047.

[13] K. S. Suslick, “Sonochemistry,” *Science*, vol. 247, no. 4949, pp. 1439–1445, 1990.

[14] M. S. Strano, V. C. Moore, M. K. Miller, M. J. Allen, E. H. Haroz, C. Kittrell, *et al.*, “The Role of Surfactant Adsoprtion during Ultrasonication in the Dispersion of Single-Walled Carbon Nanotubes,” *Journal of Nanoscience and Nanotechnology*, vol. 3, no. 1–2, pp. 81–86, 2003, doi: DOI: info:doi/10.1166/jnn.2003.194.

[15] E. A. Zakharychev, M. A. Kabina, E. N. Razov, and L. L. Semenycheva, “A study of the stability of aqueous suspensions of functionalized carbon nanotubes,” *Colloid J.*, vol. 78, no. 5, pp. 602–607, 2016, doi: 10.1134/S1061933X16050240.

[16] Y. Bai, F. Wu, D. Lin, and B. Xing, “Aqueous stabilization of carbon nanotubes: effects of surface oxidization and solution chemistry,” *Environ. Sci. Pollut. Res.*, vol. 21, no. 6, pp. 4358–4365, 2014, doi: 10.1007/s11356-013-2304-7.

[17] O. S. Zueva, O. N. Makshakova, B. Z. Idiyatullin, D. A. Faizullin, N. N. Benevolenskaya, A. O. Borovskaya, *et al.*, “Structure and properties of aqueous dispersions of sodium dodecyl sulfate with carbon nanotubes,” *Russ. Chem. Bull.*, vol. 65, no. 5, pp. 1208–1215, 2016, doi: 10.1007/s11172-016-1437-5.

[18] N. Grossiord, O. Regev, J. Loos, J. Meuldijk, and C. E. Koning, “Time-Dependent Study of the Exfoliation Process of Carbon Nanotubes in Aqueous Dispersions by Using

UV−Visible Spectroscopy," *Anal. Chem.*, vol. 77, no. 16, pp. 5135–5139, 2005, doi: 10.1021/ac050358j.

[19] M. J. O'Connell, S. M. Bachilo, C. B. Huffman, V. C. Moore, M. S. Strano, E. H. Haroz, *et al.*, "Band Gap Fluorescence from Individual Single-Walled Carbon Nanotubes," *Science*, vol. 297, no. 5581, pp. 593–596, 2002, doi: 10.1126/science.1072631.

[20] K. Yurekli, C. A. Mitchell, and R. Krishnamoorti, "Small-Angle Neutron Scattering from Surfactant-Assisted Aqueous Dispersions of Carbon Nanotubes," *J. Am. Chem. Soc.*, vol. 126, no. 32, pp. 9902–9903, 2004, doi: 10.1021/ja047451u.

[21] L. Jiang, L. Gao, and J. Sun, "Production of aqueous colloidal dispersions of carbon nanotubes," *J. Colloid Interface Sci.*, vol. 260, no. 1, pp. 89–94, 2003, doi: 10.1016/S0021-9797(02)00176-5.

[22] J. Rausch, R.-C. Zhuang, and E. Mäder, "Surfactant assisted dispersion of functionalized multi-walled carbon nanotubes in aqueous media," *Compos. Part Appl. Sci. Manuf.*, vol. 41, no. 9, pp. 1038–1046, 2010, doi: 10.1016/j.compositesa.2010.03.007.

[23] C. Richard, F. Balavoine, P. Schultz, T. W. Ebbesen, and C. Mioskowski, "Supramolecular Self-Assembly of Lipid Derivatives on Carbon Nanotubes," *Science*, vol. 300, no. 5620, pp. 775–778, 2003, doi: 10.1126/science.1080848.

[24] Y. N. Tolchkov, Z. A. Mikhaleva, R. D. A. Sldozian, N. R. Memetov, and A. G. Tkachev, "Effect of Surfactant Stabilizers on the Distribution of Carbon Nanotubes in Aqueous Media," *J. Wuhan Univ. Technol.-Mater Sci Ed*, vol. 33, no. 3, pp. 533–536, 2018, doi: 10.1007/s11595-018-1855-3.

[25] E. Ramos, W. A. Pardo, M. Mir, and J. Samitier, "Dependence of carbon nanotubes dispersion kinetics on surfactants," *Nanotechnology*, vol. 28, no. 13, p. 135702, 2017, doi: 10.1088/1361-6528/aa5dd4.

[26] T. P. Teng, Y. B. Fang, Y. C. Hsu, and L. Lin, "Evaluating Stability of Aqueous Multiwalled Carbon Nanotube Nanofluids by Using Different Stabilizers," *Journal of Nanomaterials*, vol. 2014, 2014.

[27] S. Javadian, A. Motaee, M. Sharifi, H. Aghdastinat, and F. Taghavi, "Dispersion stability of multi-walled carbon nanotubes in catanionic surfactant mixtures," *Colloids Surf. Physicochem. Eng. Asp.*, vol. 531, pp. 141–149, 2017, doi: 10.1016/j.colsurfa.2017.07.081.

[28] B. White, S. Banerjee, S. O'Brien, N. J. Turro, and I. P. Herman, "Zeta-Potential Measurements of Surfactant-Wrapped Individual Single-Walled Carbon Nanotubes," *J. Phys. Chem. C*, vol. 111, no. 37, pp. 13684–13690, 2007, doi: 10.1021/jp070853e.

[29] K. B. Shelimov, R. O. Esenaliev, A. G. Rinzler, C. B. Huffman, and R. E. Smalley, “Purification of single-wall carbon nanotubes by ultrasonically assisted filtration,” *Chem. Phys. Lett.*, vol. 282, no. 5, pp. 429–434, 1998, doi: 10.1016/S0009-2614(97)01265-7.

[30] K. L. Lu, R. M. Lago, Y. K. Chen, M. L. H. Green, P. J. F. Harris, and S. C. Tsang, “Mechanical damage of carbon nanotubes by ultrasound,” *Carbon*, vol. 34, no. 6, pp. 814–816, 1996, doi: 10.1016/0008-6223(96)89470-X.

[31] Q. Li, Y. Ma, C. Mao, and C. Wu, “Grafting modification and structural degradation of multi-walled carbon nanotubes under the effect of ultrasonics sonochemistry,” *Ultrason. Sonochem.*, vol. 16, no. 6, pp. 752–757, 2009, doi: 10.1016/j.ultsonch.2009.03.006.

[32] J. Yu, N. Grossiord, C. E. Koning, and J. Loos, “Controlling the dispersion of multi-wall carbon nanotubes in aqueous surfactant solution,” *Carbon*, vol. 45, no. 3, pp. 618–623, 2007, doi: 10.1016/j.carbon.2006.10.010.

[33] J. L. Bahr, E. T. Mickelson, M. J. Bronikowski, R. E. Smalley, and J. M. Tour, “Dissolution of small diameter single-wall carbon nanotubes in organic solvents?,” *Chem. Commun.*, no. 2, pp. 193–194, 2001, doi: 10.1039/B008042J.

[34] S. A. Ntim, O. Sae-Khow, C. Desai, F. A. Witzmann, and S. Mitra, “Size dependent aqueous dispersibility of carboxylated multiwall carbon nanotubes,” *J. Environ. Monit.*, vol. 14, no. 10, pp. 2772–2779, 2012, doi: 10.1039/C2EM30405H.

[35] Z. Wu and S. Mitra, “Length reduction of multi-walled carbon nanotubes via high energy ultrasonication and its effect on their dispersibility,” *J. Nanoparticle Res.*, vol. 16, no. 8, p. 2563, 2014, doi: 10.1007/s11051-014-2563-3.

[36] B. Krause, M. Mende, P. Pötschke, and G. Petzold, “Dispersability and particle size distribution of CNT in an aqueous surfactant dispersion as a function of ultrasonic treatment time,” *Carbon*, vol. 48, no. 10, pp. 2746–2754, 2010, doi: 10.1016/j.carbon.2010.04.002.

[37] J. M. Vallerot, X. Bourrat, A. Mouchon, and G. Chollon, “Quantitative structural and textural assessment of laminar pyrocarbons through Raman spectroscopy, electron diffraction and few other techniques,” *Carbon*, vol. 44, no. 9, pp. 1833–1844, 2006, doi: 10.1016/j.carbon.2005.12.029.

[38] H. Kataura, Y. Kumazawa, Y. Maniwa, I. Umezu, S. Suzuki, Y. Ohtsuka, *et al.*, “Optical properties of single-wall carbon nanotubes,” *Synth. Met.*, vol. 103, no. 1, pp. 2555–2558, 1999, doi: 10.1016/S0379-6779(98)00278-1.

[39] R. Rastogi, R. Kaushal, S. K. Tripathi, A. L. Sharma, and I. Kaur, “Comparative study of carbon nanotube dispersion using surfactants,” *Journal of Colloid and Interface Science*, vol. 328, no. 2, pp. 421–428, 2008.

[40] M. D. Clark, S. Subramanian, and R. Krishnamoorti, “Understanding surfactant aided aqueous dispersion of multi-walled carbon nanotubes,” *J. Colloid Interface Sci.*, vol. 354, no. 1, pp. 144–151, 2011, doi: 10.1016/j.jcis.2010.10.027.

[41] Z. F. Li, G. H. Luo, W. P. Zhou, F. Wei, R. Xiang, and Y. P. Liu, “The quantitative characterization of the concentration and dispersion of multi-walled carbon nanotubes in suspension by spectrophotometry,” *Nanotechnology*, vol. 17, no. 15, pp. 3692–3698, 2006, doi: 10.1088/0957-4484/17/15/012.

[42] D. Baskaran, J. W. Mays, and M. S. Bratcher, “Noncovalent and Nonspecific Molecular Interactions of Polymers with Multiwalled Carbon Nanotubes,” *Chem. Mater.*, vol. 17, no. 13, pp. 3389–3397, 2005, doi: 10.1021/cm047866e.

[43] P. Düngen, M. Prenzel, C. V. Stappen, N. Pfänder, S. Heumann, and R. Schlögl, “Investigation of Different Pre-Treated Multi-Walled Carbon Nanotubes by Raman Spectroscopy,” *Mater. Sci. Appl.*, vol. 8, no. 8, pp. 628–641, 2017, doi: 10.4236/msa.2017.88044.

[44] A. Sadezky, H. Muckenhuber, H. Grothe, R. Niessner, and U. Pöschl, “Raman microspectroscopy of soot and related carbonaceous materials: Spectral analysis and structural information,” *Carbon*, vol. 43, no. 8, pp. 1731–1742, 2005, doi: 10.1016/j.carbon.2005.02.018.